DOI: 10.1002/chem.201101837

Gold Nanoparticles Stabilized by Thioether Dendrimers

Jens Peter Hermes,[a] Fabian Sander,[a] Torsten Peterle,[a, b] Raphael Urbani,[c] Thomas Pfohl,[c] Damien Thompson,[d] and Marcel Mayor*[a, e]

Abstract: Ligand-stabilized gold nanoparticles (Au NPs) are promising materials for nanotechnology with applications in electronics, catalysis, and sensors. These applications depend on the ability to synthesize stable and monodisperse NPs. Herein, the design and synthesis of two series of dendritic thioether ligands and their ability to stabilize Au NPs is presented. The dendrimers have 1,3,5-trisubstituted benzene branching units bridged by either *meta*-xylene or ethylene moieties. A comparison between the two ligands shows how both size control and the stability of the NPs are influenced by the nature of the ligand–NP wrapping interaction. The *meta*-xylene-bridged ligands provided NPs with a narrow size distribution centered around a diameter of 1.2 nm, whereas the NPs formed with ethylene-bridged dendrimers lack long-term stability with NP aggregation detected by UV/Vis spectroscopy and transmission electron microscopy. The bulkier *tert*-butyl-functionalized *meta*-xylene bridges form larger ligand shells that inhibit further growth of the NPs and thus provide a simple route to stable and monodisperse Au NPs that may find use as functional components in nanoelectronic devices.

Keywords: dendrimers · gold · ligand design · nanoparticles · thioethers

Introduction

The research field of gold nanoparticles (Au NPs) has been steadily advancing in the past decade. The chemical stability and size-dependent properties of Au NPs make them attractive materials for use in nanotechnology.[1–4] The scope of future applications is broad,[1] ranging from advanced electronic[5–9] and photonic[10,11] devices to ultrasensitive chemical[12–16] and biological sensors.[17] In addition, Au NPs have current and potential applications in biological labeling,[18–22] medical diagnostics,[23] and catalysis.[24,25] Aqueous Au NPs are often formed as citrate-stabilized NPs and then functionalized by using peptides[26,27] or DNA.[20,21] However, within this study we focused on nonpolar organic solvents in which mainly alkanethiols have been used to stabilize Au NPs, an approach widely used since the pioneering work of Brust et al.[28] In addition to free thiols, the less reactive thioethers have also been used to ligate NP surfaces.[29–34] The thioether–gold coordination is much weaker than the covalent thiolate–gold interaction.[35] Therefore multidentate thioether ligands may be used to form self-assembled, multivalent—bound, stable and monodisperse ligand-wrapped NPs with a distinct low-integer number of ligands wrapping and effectively ensnaring each NP.[31–33] The first application of multidentate macromolecular ligands for the stabilization of Au NPs was the use of thioether polymers.[36–39] The use of thioether dendrimers as stabilizing ligands has also been reported.[40–43] The advantage of dendrimers over polymers is the control over their monodispersity. The molecular structures of reported dendritic ligands vary from stiff arylic sulfides[40,41] to partially flexible benzylic/arylic sulfides[42] and highly flexible benzylic thioether dendrimers.[43] Superior stability and monodispersity has been reported for the latter. Unfortunately, one cannot unambiguously relate these findings to thioether properties as the presence of additional ether moieties may have played a role, with recent work showing that ether moieties present in poly(ethylene glycol) (PEG) dendrimers are also able to stabilize Au NPs.[44] Other known stabilizing units for the formation of dendrimer-encapsulated metal NPs are poly(amidoamine) (PAMAM)[45–47] and poly(propyleneimine) (PPI) structures.[48,49] Thioether dendrimers used for applications other than the stabilization of NPs have also been reported.[50–53]

The goal of this work was to develop dendritic thioether structures that are able to stabilize Au NPs with monodisperse size through the formation of NP–ligand complexes that allow a low-integer number of ligands to cover each NP

[a] J. P. Hermes, F. Sander, Dr. T. Peterle, Prof. Dr. M. Mayor
Department of Chemistry, University of Basel
St. Johanns-Ring 19, 4056 Basel (Switzerland)
E-mail: marcel.mayor@unibas.ch

[b] Dr. T. Peterle
Evonik Degussa GmbH
Untere Kanalstraße 3, 79618 Rheinfelden (Germany)

[c] R. Urbani, Prof. Dr. T. Pfohl
Department of Chemistry, University of Basel
Klingelbergstrasse 80, 4056 Basel (Switzerland)

[d] Dr. D. Thompson
Theory Modelling and Design Centre, Tyndall National Institute
Lee Maltings, University College Cork, Cork (Ireland)

[e] Prof. Dr. M. Mayor
Institute of Nanotechnology, Karlsruhe Institute of Technology (KIT)
P.O. Box 3640, 76021 Karlsruhe (Germany)

Supporting information for this article is available on the WWW under http://dx.doi.org/10.1002/chem.201101837.

while also providing the long-term stability that is a prerequisite for technological applications. Dendrimers are ideal candidate ligands with their branched, flexible architecture potentially allowing for extensive NP surface coverage and therefore providing monodisperse NPs that do not aggregate over time. The two dendritic ligands synthesized in this work are both based on benzylic thioethers, the combination of flexibility and weak individual thioether anchoring groups providing a multivalent ligand for the assembly of NPs complexed by a low number of ligands. Different generations and structural motifs of the dendritic ligands were synthesized to determine their NP-stabilizing abilities and their influence on the size distributions of the NPs obtained. The NPs were investigated by UV/Vis and ^{1}H NMR spectroscopy, thermogravimetric analysis (TGA), small-angle X-ray scattering (SAXS), and both standard transmission electron microscopy (TEM) and high-resolution scanning transmission electron microscopy (HRSTEM).

Results and Discussion

Concept and strategy: We have recently shown that linear, unbranched thioether ligands with a certain threshold length are able to stabilize Au NPs and provide a narrow size distribution of NPs with a diameter of around 1.1 nm that do not aggregate over time.[31–33] These linear thioethers are oligomeric structures constructed from a *meta*-xylene-bridged thioether motif. In this work we designed and synthesized two series of dendritic thioether ligands (Scheme 1 and Scheme 2) and investigated their potential for stabilizing Au NPs. The dendrimers were synthesized by a convergent approach. The dendrons were synthesized by starting from the terminal groups and working back towards the central unit. The dendritic ligands are branched with a 1,3,5-trisubstituted benzene. The use of benzylic thioethers should give flexible molecular structures that allow all three sulfide groups to be orientated towards the NP surface. Note that a similar building block has already been reported to stabilize Au_{55}.[54] The dendrimers differ by the bridging unit that separates the branching units from each other. The nomenclature of the ligands emphasizes the different bridging units, which are a focus of this work. The bridges were introduced into the ligand design to 1) provide more separated thioether anchoring points and 2) to increase the amount of free space in the center of the dendrimers. This reduced branching density should improve the ability of the dendrimers to adapt to the convex NP surface by forming a concave pocket. We thus hypothesized considerably improved wrapping features for such dendrimers with "diluted" branching units. The first series (***m*X** ligands, Scheme 1) use a *tert*-butyl-functionalized *meta*-xylene to interconnect two sulfur atoms, the same moieties used for the previously studied linear ligands.[31–33] The second series (**Et** ligands, Scheme 2) uses ethylene bridges for the interconnection of two neighboring sulfur atoms. Two generations of dendrimers were synthesized for each dendrimer series to investigate the correlation between dendrimer generation and stabilizing or size-steering features.

Ligand synthesis: The synthesis of the ***m*X** dendrimers is shown in Scheme 1. The basic building blocks **1** and **4** were synthesized by using literature protocols.[55,56] The branching unit **2** was obtained after substitution of the bromides of starting material **1** with lithium chloride in dimethylforma-

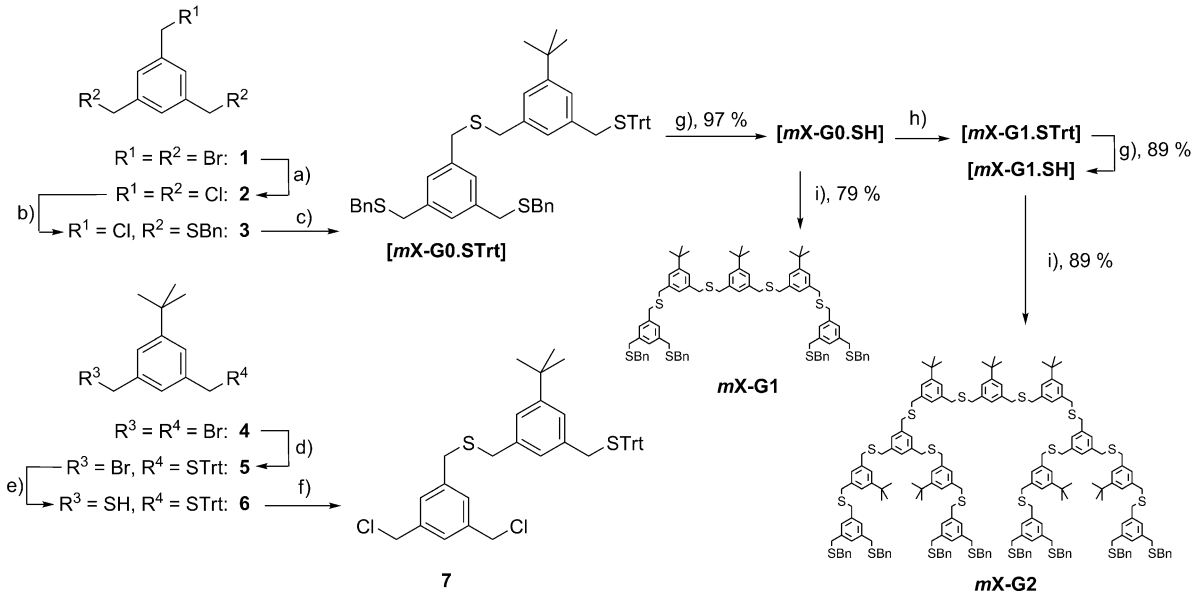

Scheme 1. Synthesis of α,α′-*meta*-xylene-bridged dendrons and dendrimers of various generations. Reagents and conditions: a) LiCl, DMF, 0 °C, 30 min, RT, 2 h, 90%; b) BnSH, NaH, THF, RT, 1 h, 44%; c) **6**, NaH, THF, RT, 1 h, 99%; d) TrtSH, NaH, THF, RT, 2 h, 49%; e) 1. KSAc, THF, RT, 1 h; 2. MeOH, K_2CO_3, RT, 1 h, 80%; f) **2**, NaH, THF, RT, 2 h, 49%; g) TFA, Et_3SiH, CH_2Cl_2, RT, 15 min; h) **7**, NaH, THF, RT, 1 h, 90%; i) **4**, NaH, THF, RT, 1 h.

mide (DMF). The bromides were substituted because chlorides are more stable in the presence of protected thiols. The dendron terminal unit **3** was synthesized by statistical nucleophilic substitution with benzyl mercaptan (BnSH) and sodium hydride (NaH) as base in tetrahydrofuran (THF). The G0 dendron **[*m*X-G0.STrt]** was formed from the terminal unit **3** with the monothiol **6**. Compound **6** was prepared from the monofunctionalized bromide **5** by a mild one-pot procedure for the conversion of benzylic bromides into thiols.[57] After deprotection of the trityl group with trifluoroacetic acid (TFA), the **[*m*X-G0.SH]** dendron can be extended by branching unit **7** to the next generation dendron. Precursor **7** was assembled from the bridging unit **6** with an excess of the dendritic branching unit **2**. The respective **[*m*X-G*n*.SH]** dendrons were used to form the final dendrimers ***m*X-G1** and ***m*X-G2** with central unit **4**. In view of the statistical nature of some monofunctionalizations, all the reactions gave good-to-excellent yields.

Scheme 2 depicts the synthesis of the **Et** dendrons. The first dendron **[Et-G0.STrt]** was synthesized starting from thiirane (ethylene sulfide). The bridging unit **8** was synthesized by ring-opening of thiirane with an excess of trityl thiol (TrtSH) in the presence of triethylamine (TEA) as base. As for the ***m*X** ligands, subsequent nucleophilic substitution and deprotection reactions of the trityl groups led to the terminal thiols as powerful nucleophiles. All the reactions gave good-to-excellent yields considering the statistical nature of the monofunctionalization reactions.

Ligand-stabilized nanoparticles: Au NPs were prepared in the presence of the dendritic thioether ligands ***m*X-G*n*** and **Et-G*n*** to investigate the ability of these ligands to stabilize NPs by preventing aggregation. The NPs were prepared in a two-phase water/dichloromethane system closely following the procedure developed by Brust et al.[28] (see the Experimental Section for the synthetic protocol). The gold(III) precursor, tetrachloroauric acid, dissolved in water was transferred to the organic phase by tetra-*n*-octylammonium bromide (TOAB). To keep the ratio between the gold(III) precursor and thioether moieties comparable to earlier studies,[31–33] the amount of added ligand was normalized to the number of thioether groups. The starting point for investigating the ability of a ligand to stabilize Au NPs was in all cases equal numbers of ligand sulfur atoms and gold atoms in the precursor. Thus, an eight-fold excess of the gold(III) precursor was used for ***m*X-G1** and a twenty-fold excess was used for ***m*X-G2**. Although for these ***m*X** ligands the ratios were maintained, the concentration of the ligand was raised in the case of the **Et** ligands. The reduction of gold(III) in the presence of the thioether ligands was carried out by quickly adding an aqueous solution of sodium borohydride to the two-phase system. After aqueous workup, the organic phases were dried over $MgSO_4$ and filtered.

In the case of the ***m*X** ligands, the change in color to dark brown indicated the formation of the NPs **Au-*m*X-G1** and **Au-*m*X-G2**. Precipitation of gold was not observed, which indicates an efficient stabilization of the Au NPs formed. In analogy to linear oligomers,[31–33] coating by ***m*X** ligands provided the NPs with enough stability to allow removal of TOAB by applying a precipitation and centrifugation protocol[32] and of the excess ligand by size exclusion chromatography (SEC). Analysis by ^{1}H NMR spectroscopy (see Figure S1 in the Supporting Information, SI) corroborated the total removal of TOAB. The spectra also showed the presence of surface-bound dendrimer ligands, corroborating their stabilizing nature as a coating of NPs. As far as the gold atoms were concerned, the synthetic procedure and removal of TOAB led to the formation of NPs in a yield of around 95%. However, approximately 10–20% of the NPs were lost during SEC because some late SEC vials still showed the presence of excess ligand and were therefore discarded to obtain only ligand-stabilized NPs. This loss is due

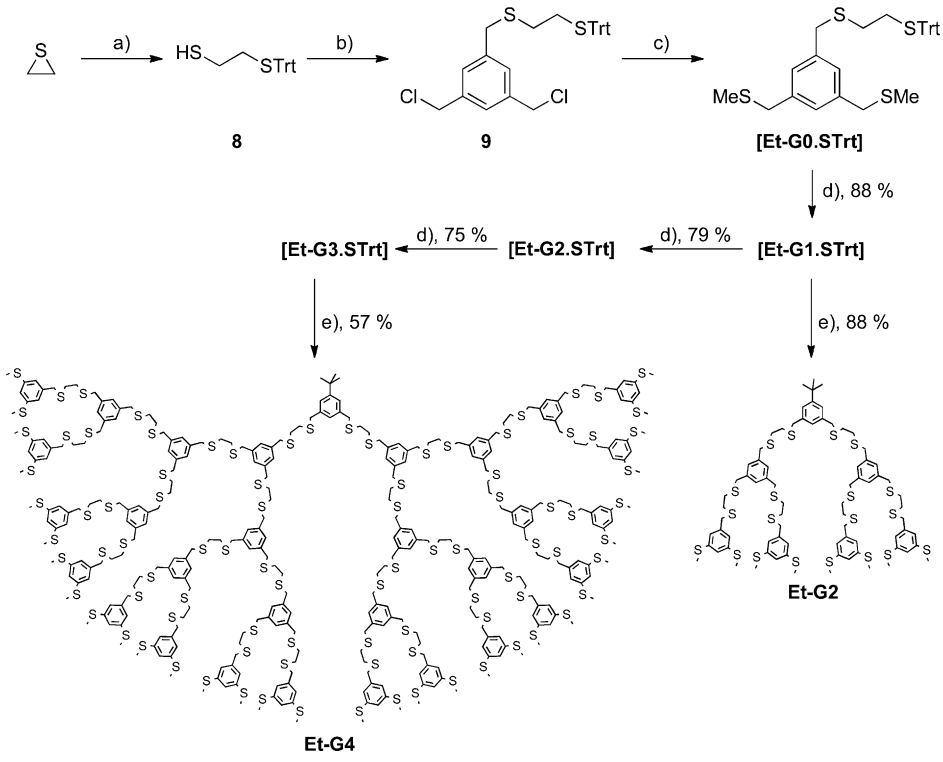

Scheme 2. Synthesis of ethylene-bridged dendrons and dendrimers of various generations. Reagents and conditions: a) TrtSH, TEA, DMF, RT, 92%; b) **2**, K_2CO_3, THF, reflux, 46%; c) NaSMe, DMF, RT, 88%; d) 1. Et_3SiH, TFA, CH_2Cl_2, RT; 2. **9**, NaH, THF, RT; e) 1. Et_3SiH, TFA, CH_2Cl_2, RT; 2. **4**, NaH, THF, RT, 1 h.

to the overlap in the retention times of ligand-stabilized NPs and the free ligand.

The formation of NPs in the presence of **Et-G2** led to immediate and complete precipitation of aggregated NPs after addition of the reducing agent. The 1:1 ratio of gold equivalents to sulfur atoms in the ligand design used initially was then adjusted to a ratio of 1:2. A quick and complete precipitation of aggregated NPs was still observed. The same 1:2 ratio was used during the formation of NPs in the presence of the fourth generation ligand **Et-G4**. In this case, upon addition of the reducing agent, the organic phase turned a reddish brown color pointing to the formation of stable NPs; the precipitation of NPs was not observed for **Et-G4**.

To analyze the ligand-stabilized NPs UV/Vis spectra were recorded (Figure 1). In the case of the stable and redissolvable ***m*X**-ligand-stabilized NPs new solutions were prepared from dried NPs in CH_2Cl_2, whereas in the case of **Et-G4**-stabilized NPs, the organic layer was investigated directly by UV/Vis spectroscopy. The organic layer of **Au-Et-G4** showed a weak plasmon resonance band, which indicates a NP distribution comprising a few NPs with diameters of around 2 nm from the very beginning (Figure 1A, black line). A color change from reddish brown to dark red was observed upon storing the isolated and dried organic phase under ambient conditions in CH_2Cl_2 in the presence of excess ligand for several weeks. As shown in Figure 1A (gray line), a prominent plasmon resonance band was observed after 4 weeks, which indicates an increase in NP size upon storage. Interestingly, in spite of this aggregation of initially formed NPs to give larger NPs, the precipitation of aggregated NPs was not observed.

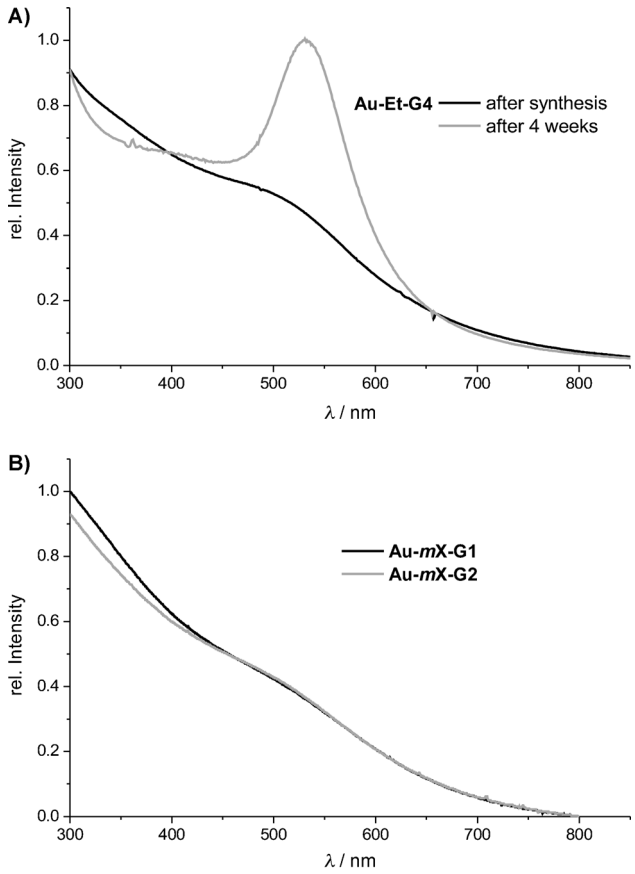

Figure 1. UV/Vis absorption spectra in CH_2Cl_2 of ligand-stabilized Au NPs. A) Spectra of **Au-Et-G4** NPs directly after NP formation (black) and after 4 weeks (gray) in CH_2Cl_2. The arising plasmon resonance band indicates the aggregation of NPs. B) Spectra of **Au-*m*X-G1** (black) and **Au-*m*X-G2** (gray). The spectra are normalized to match at 520 nm. The weak plasmon resonance peaks indicate NPs with diameters of around and below 1.6 nm.[59]

The weak plasmon resonance band in the UV/Vis spectra of both the ***m*X-G1**- and ***m*X-G2**-stabilized NPs (Figure 1B) point to NP sizes of around and below 1.6 nm.[58,59] The two samples show similar absorption spectra. The minor differences between 300 and 400 nm may be ascribed to the presence of different amounts of excess ligand. Interestingly, these UV/Vis spectra remained unchanged when the solutions were retested after 6 months, which indicates the excellent long-term stability of ***m*X**-ligand-stabilized NPs even on exposure to air and light. However, higher temperatures than room temperature were avoided as a slight growth of NPs has previously been reported at temperatures of around 40 °C.[31]

HRSTEM analysis of the **Et**-ligand-stabilized NPs and TEM analysis of the ***m*X**-ligand-stabilized NPs were performed to determine the diameters (sizes) of the NPs formed. Micrographs were taken of CH_2Cl_2 solutions of NPs deposited on carbon-coated copper grids (Figure 2). Large differences between the **Et-G4**- (Figure 2A) and ***m*X**-ligand-stabilized NPs (Figure 2B and C) are readily visible to the naked eye. A solution of CH_2Cl_2, aged for 4 weeks, was deposited on the carbon grid (Figure 2A) and the diameters of about 500 **Au-Et-G4** NPs were measured. As expected on the basis of the UV/Vis investigation, rather large NPs with diameters of up to 15 nm were observed. Analysis of the observed size distribution (Figure 3A) revealed a large dispersity of 1–15 nm. The broad distribution of **Au-Et-G4** NPs has a mean value of 6.2 nm with a standard deviation of ±2.4 nm. Although the NP growth of **Au-Et-G4** is interesting, we did not investigate it further because nanoelectronic device components require NPs with a distinct number of ligands for further coupling to organic–inorganic superstructures.[32,33] In contrast to these large NPs stabilized by the **Et-G4** dendrimer, very different NP diameters were observed for the ***m*X-G*n***-stabilized NPs. In this case the recorded TEM micrographs were analyzed by an automated procedure using imageJ[60] (see the SI for a detailed description). The size distributions for both NPs are displayed in Figure 3B and C. Interestingly, within the precision of the measurement, similar NP sizes of 1.1±0.3 nm and 1.2± 0.4 nm were determined for **Au-*m*X-G1** and **Au-*m*X-G2**, respectively.

The diameters of the NPs were also analyzed by SAXS, performed by dissolving the Au NPs in benzene. The 2D scattering signal was integrated to obtain intensity profiles, which are shown as log–log representations in Figure 4. The plots of **Au-*m*X-G1** and **Au-*m*X-G2** are similar, indicating

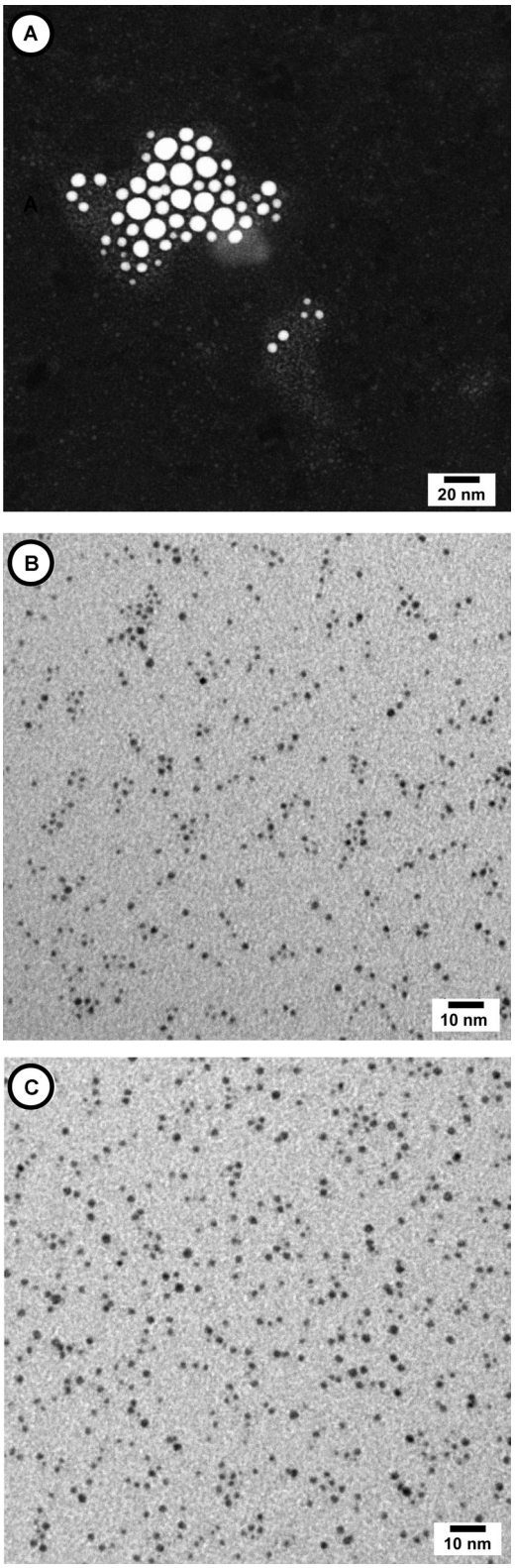

Figure 2. A) Representative HRSTEM image of **Au-Et-G4** after being dissolved in CH_2Cl_2 for 4 weeks. Representative TEM images of B) **Au-*m*X-G1** and C) **Au-*m*X-G2** NPs, respectively.

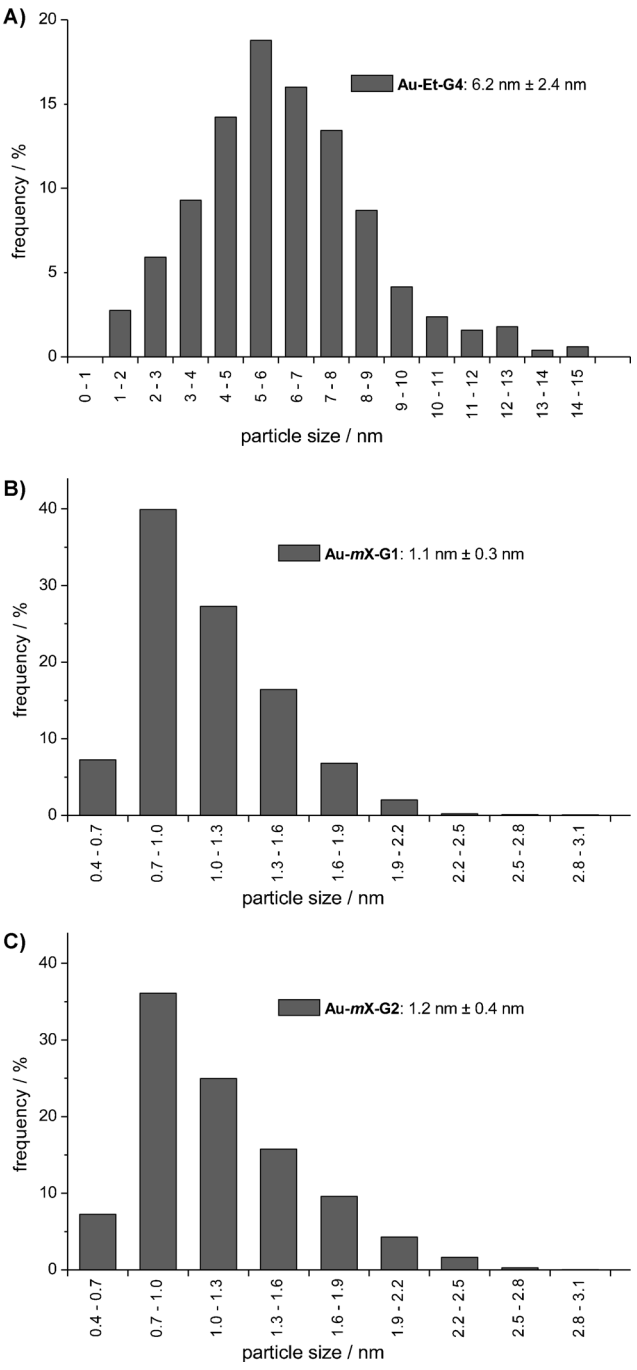

Figure 3. Size distributions of ligand-stabilized Au NPs: A) **Au-Et-G4** after storage in solution (500 NPs were measured manually), B) **Au-*m*X-G1**, and C) **Au-*m*X-G2** (5000 NPs were measured automatically for B and C).

similar NP sizes, as expected on the basis of TEM investigations. The shapes of the plots suggest form factors for spheres. The intensity plots were fitted with Nanofit software version 1.2 from Bruker, using a least-squares method for polydisperse, spherical particles. The analysis revealed both samples to have diameters of around 1.6 nm by assuming a Gaussian distribution of the NP diameters of $\sigma =$ 0.4 nm.

The diameters of the NPs measured by small-angle X-ray scattering (SAXS) differ from the values found in TEM in-

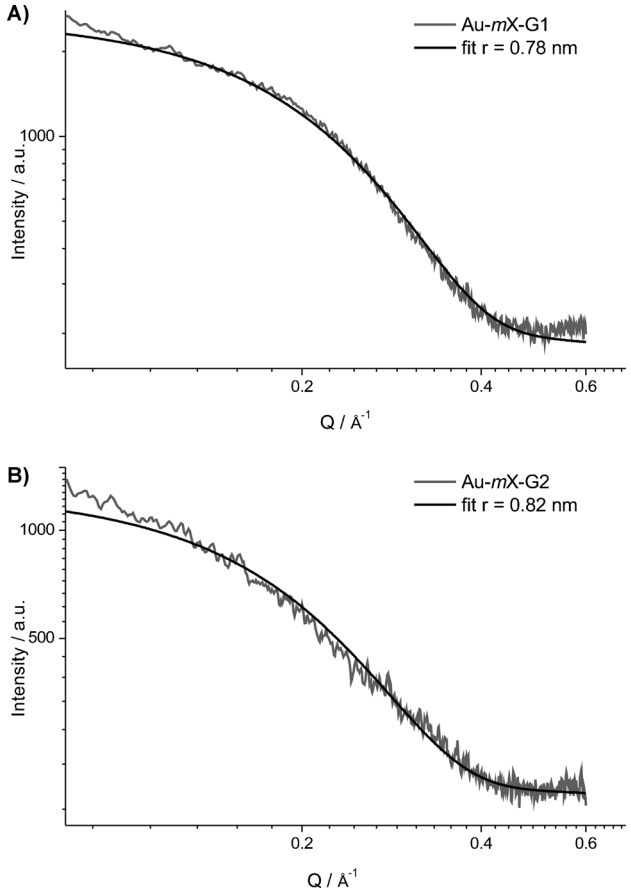

Figure 4. SAXS intensity plots as log–log representations and best fits for A) **Au-*m*X-G1** and B) **Au-*m*X-G2**.

vestigations (diameters 1.1 and 1.2 nm). This deviation has only recently been reported[33] and may be due to a slight growth of the Au NPs triggered by the X-ray irradiation; similar thermal expansion has previously been reported.[31] In addition, the organic ligand shell might add to the scattering signal leading to larger radii. Although the SAXS measurements corroborate the similarity of the sizes of both NPs, the deviation from the diameters measured by TEM is not yet understood and is the topic of further investigations. Our previous studies relied on diameters measured by TEM assuming ligand coating, which were corroborated by the chemical behavior of these NPs.[32,33] We thus currently prefer to refer to the diameters obtained by TEM over those measured by SAXS to allow comparison between the results obtained.

Despite the considerable increase in the number of sulfide groups from eight for the dendritic ligand ***m*X-G1** to twenty for ***m*X-G2**, similar NP sizes were stabilized, as found by TEM and SAXS analyses. This indicates that increasing the dendrimer generation from G1 to G2 has no significant influence on the size of the NP obtained. It rather seems that NPs grow until they reach a size that allows their enwrapping by the dendritic ligand. However, with more than twice the number of sulfide groups, the dendritic ligand ***m*X-G2** should be able to coat a considerably larger surface area than ***m*X-G1**.The ratio of organic ligand to gold should give a closer insight into the assembly of the NP and ligand shell. The excess ligand was first removed by SEC. Small amounts of dried NPs were then studied by thermogravimetric analysis (TGA). The sample was heated up to 900 °C to remove all organic components. The results for **Au-*m*X-G1** and **Au-*m*X-G2** are shown in Figure 5. The weight loss for both samples follows the same trend. Decomposition starts at around 200 °C and reaches a plateau between 600 and 700 °C. The weight loss is attributed to the decomposition and removal of the organic shell from the NP surface and the plateau is interpreted as the end of this process, when all the organic coating has been removed. Comparable weight losses of 26 and 23 % were measured for **Au-*m*X-G1** and **Au-*m*X-G2**, respectively.

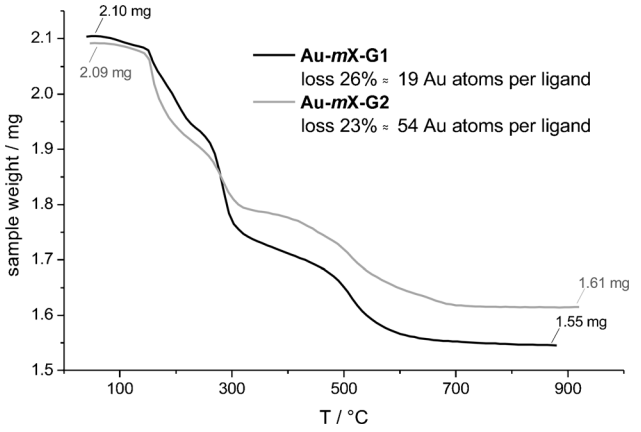

Figure 5. Thermogravimetric analyses of **Au-*m*X-G1** (black) and **Au-*m*X-G2** (gray).

Knowing the size of the NPs from the TEM investigations allows calculation of their mass and thus the average mass of ligand coating per NP can be estimated from the weight percentage obtained by TGA. First, the mass of gold per ligand is derived from the rule of proportion from the mass of the ligand and the mass percentage of both the gold and ligand [Eq. (1) in the SI]. This value is divided by the molecular mass of gold to obtain the number of gold atoms per ligand [Eq. (2) in the SI]. For the **Au-*m*X-G1** NPs a ratio of 19 gold atoms per ***m*X-G1** ligand was obtained. By using the density of bulk gold (ρ_{Au}) the number of gold atoms per NP was estimated to be 41 for NPs with an average diameter of 1.1 nm (from TEM). The calculated 19 gold atoms per octadentate ***m*X-G1** ligand indicate a ratio of two ***m*X-G1** ligands per gold NP. A similar pairwise coating of the NP surface has been observed for linear octadentate ligands.[32,33]

For the **Au-*m*X-G2** NPs, the ratio of gold atoms per ***m*X-G2** ligand was determined to be 54. The number of gold atoms per 1.2 nm NP was calculated to be 53 atoms on average, which indicates that a single ***m*X-G2** ligand can stabilize the entire 1.2 nm NP. Note that Au_{55} clusters are known to have a diameter of 1.4 nm.[8] The calculation with ρ_{Au} seems

to overestimate the number of gold atoms in the NP. As the sizes of the NPs determined by TEM are smaller than those determined by SAXS studies, this overestimation to some extent compensates the deviation in size. In view of the extended structure of the ***m*X-G2** ligand with more than twice the number of phenyl subunits and sulfide groups compared with the first generation analogue ***m*X-G1**, this ability to enwrap the entire surface of a NP of comparable size is not surprising. This specific ratio of one ligand stabilizing one NP is very rare. To our knowledge this has only been achieved by the use of a single polymer chain[61] or by radical-chain polymerization on the NP surface.[62]

A molecular dynamics model of a Au_{55} cluster coated with ***m*X-G2** is depicted in Figure 6. The greed of the sulfide groups for noble metal surfaces guarantees the adhesion of the branched ligand structure to the NP surface and the considerable dimension of the ligand only allows for a single ligand per NP in the case of **Au-*m*X-G2**. As the thioether–gold bond is weak we can expect that the NP–ligand assembly does not contain any "staples", which have been found in the crystal structures of several thiol-stabilized Au NPs.[63,64] The discrete and integer number of ligands per NP may even allow use of the supramolecular notations $Au_{41}\subset$-(***m*X-G1**)$_2$ and $Au_{53}\subset$***m*X-G2** for the NPs **Au-*m*X-G1** and **Au-*m*X-G2**, respectively. However, this notation is misleading as it suggests that the number of gold atoms forming the NPs is not controlled. In view of the NP size distributions displayed in Figure 3B and C, a more appropriate description would be $Au_{41\pm8}\subset$(***m*X-G1**)$_2$ and $Au_{53\pm10}\subset$***m*X-G2**, respectively. To avoid confusion we prefer the old notations **Au-*m*X-G1** and **Au-*m*X-G2**, respectively.

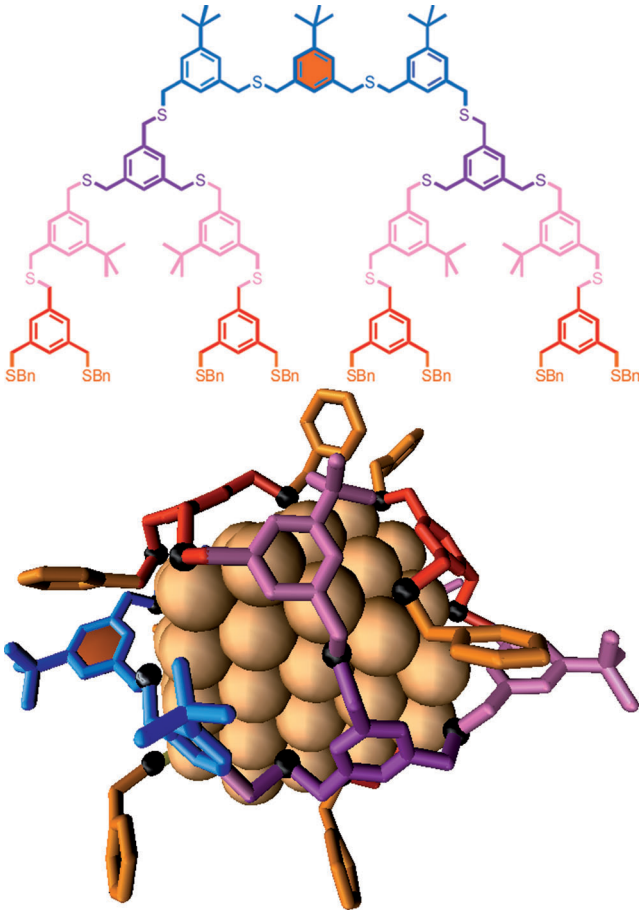

Figure 6. Quantum mechanical calculations of thioether–gold bond strengths were combined with a classical molecular dynamics model to calculate one-dendrimer (shown) and alternative two-dendrimer complexes with the Au NP, modeled to a first approximation by a 55-atom cluster (diameter 1.4 nm)[8] in dichloromethane. The details of the calculations will be presented elsewhere.[65] The calculations indicate that the alternative two-dendrimer state is less stable for these sized NPs. The low likelihood of replacement of the fully bound single dendrimer by two partially bound dendrimers was determined by using an energy function summed over beneficial wrapping interactions (individual thioether–gold bond strengths plus van der Waals dendrimer–gold contacts) and wrapping penalties (loss in dendrimer conformational freedom plus dendrimer and gold desolvation).

The two dendrimer structures **Et-G4** and ***m*X-G2** display large differences in the long-term stability of the coated Au NPs. Although NPs stabilized by **Et-G4** quickly aggregate to form larger NPs, ***m*X-G2**-stabilized NPs display excellent long-term stability, which makes them very interesting ligand structures for obtaining monofunctionalized NPs, for example, for use as TEM labels. As a working hypothesis we attribute this unequal long-term stability of ligand-stabilized NPs to the different bridging units. The bulky *tert*-butyl-functionalized *meta*-xylene bridges create a large ligand shell around the Au NP surface preventing further aggregation. This steric protection of the NP surface provides not only a certain size control during the growth of the NPs, but also long-term stability for the NPs **Au-*m*X-G1** and **Au-*m*X-G2**. The loss of long-term stability in the case of **Au-Et-G4** is attributed to the reduced bulkiness of the ethylene bridges in this dendritic structure. It seems that this motif is not able to provide a strong protective shell and thus NPs get close enough to aggregate. In addition, both series of dendritic ligands differ in their terminal groups: The ***m*X-Gn** series has terminal benzyl sulfides whereas the terminal groups of the **Et-Gn** series are methyl sulfides. However, the considerable differences in long-term stability probably arise from the dendritic skeleton and not from the terminal groups. This assumption is supported by a model in which the terminal benzene rings (orange) do not coordinate to the gold surface.

Conclusion

Two dendrimer motifs have been synthesized, both based on thioethers mounted on a 1,3,5-trimethylbenzene scaffold as branching units but with different spacers to "expand" the dendrimer structure. The spacer units reduce the density of the branching units and should therefore allow the dendritic ligand to adapt to the convex curvature of NPs. As spacer units, α,β-ethynyl bridges and α,α′-*meta*-xylene structures comprising a bulky *tert*-butyl group have been considered. Although from the ethynyl-bridged dendrimer the second and fourth generation ligands **Et-G2** and **Et-G4** were syn-

thesized, the first and second generation ligands ***m*X-G1** and ***m*X-G2** were prepared in the case of the *meta*-xylene spacers. The ability of these dendrimers to control the growth and to stabilize particular sizes of Au NPs was investigated by using them as reagents during the biphasic reduction of chloroauric acid. With the two ethynyl-bridged dendrimers only the larger **Et-G4** displayed some limited NP stabilizing features. **Et-G4** was neither able to control the size of NPs during their formation nor to stabilize the formed NPs in solution over time. In contrast, both *meta*-xylene-bridged dendrimers were able to stabilize small Au NPs with average diameters of between 1.1 and 1.2 nm (from TEM) in very good yields and with excellent long-term stability. The limited surface area of these small NPs allows all the thioethers of only two dendritic ligands ***m*X-G1** to coordinate to a NP. In the case of the further expanded dendrimer ***m*X-G2**, the spatial limitation only allows a single ligand to coordinate its 20 thioethers to the NP surface. Thermogravimetric analysis corroborated the expected 1:2 and 1:1 ratios between the NP and dendritic ligands ***m*X-G1** and ***m*X-G2**, respectively. The considerable increase in both the control over NP size and NP stability has been attributed to the bulkiness of the dendritic coating with a *tert*-butyl-functionalized *meta*-xylene linker, which prevents aggregation by sterically separating the metal cores of the NPs.

These NPs coated with a controlled low number of dendritic ligands may pave the way towards mono- and bifunctionalized Au NPs. We are currently investigating the potential of these organic/inorganic hybrid structures as "artificial molecules" by exploring their tolerance to wet chemical conditions.

Experimental Section

General methods and experimental procedures for all compounds are described in the Supporting Information.

Gold nanoparticle formation and purification: The Au NPs were formed on a 4–7 μmol (9–15 mg) scale with respect to dendritic ligands ***m*X-G*n*** (the same synthetic protocol was applied to **Au-Et-Gn** NPs). Chloroauric acid (***m*X-G1**: 8 equiv; ***m*X-G2**: 20 equiv) was dissolved in DI water (2 mL) and transferred to the organic phase by adding tetra-*n*-octylammonium bromide (TOAB; ***m*X-G1**: 16 equiv; ***m*X-G2**: 40 equiv) in CH_2Cl_2 (2 mL). After the addition of dendritic ligand ***m*X-G*n*** (1 equiv) in CH_2Cl_2 (2 mL) this mixture was stirred for 5 min before sodium borohydride (***m*X-G1**: 64 equiv, ***m*X-G2**: 160 equiv) was added quickly in DI water (2 mL). The color of the solution turned dark brown, which indicated the formation of Au NPs. This mixture was stirred for 15 min before the organic phase was separated; the aqueous phase was washed twice with CH_2Cl_2. The combined organic phases were dried with $MgSO_4$ and filtered. The solvent was evaporated with a stream of nitrogen or by using a rotary evaporator without heating. The dried NPs **Au-*m*X-G*n*** were redissolved in CH_2Cl_2 (< 1.5 mL) and ethanol was added (20 mL). The NPs were then precipitated by centrifugation (5 rpm, 45 min, 5 °C) to remove the TOAB. Subsequently the NPs were subjected to size exclusion chromatography (SEC) to remove excess of the ligand. Before this step, the yield of the NPs was around 95 % (based on the number of gold atoms). However, about 10–20 % of the NPs were lost during SEC because some late SEC vials still showed excess ligand and were therefore discarded. Some loss also occurred during the filtration in advance of SEC, performed to protect the column.

Acknowledgements

We gratefully acknowledge financial support by the EU through the project FUNMOL (number 213382 of the call FP7-NMP-2007-SMALL-1), the Gebert Rüf Foundation, the Swiss National Science Foundation, and the National Research Project (No. 62 Smart Materials).

[1] M. Homberger, U. Simon, *Phil. Trans. R. Soc. A* **2010**, *368*, 1405–1453.
[2] R. Sardar, A. M. Funston, P. Mulvaney, R. W. Murray, *Langmuir* **2009**, *25*, 13840–13851.
[3] M.-C. Daniel, D. Astruc, *Chem. Rev.* **2004**, *104*, 293–346.
[4] R. W. Murray, *Chem. Rev.* **2008**, *108*, 2688–2720.
[5] G. Schmid, U. Simon, *Chem. Commun.* **2005**, 697–710.
[6] R. P. Andres, J. D. Bielefeld, J. I. Henderson, D. B. Janes, V. R. Kolagunta, C. P. Kubiak, W. J. Mahoney, R. G. Osifchin, *Science* **1996**, *273*, 1690–1693.
[7] J. Liao, L. Bernard, M. Langer, C. Schönenberger, M. Calame, *Adv. Mater.* **2006**, *18*, 2444–2447.
[8] G. Schmid, *Chem. Soc. Rev.* **2008**, *37*, 1909–1930.
[9] S.-J. Kim, J.-S. Lee, *Nano Lett.* **2010**, *10*, 2884–2890.
[10] S. A. Maier, M. L. Brongersma, H. A. Atwater, *Appl. Phys. Lett.* **2001**, *78*, 16.
[11] Y. Leroux, J. C. Lacroix, C. Fave, V. Stockhausen, N. Fe'lidj, J. Grand, A. Hohenau, J. R. Krenn, *Nano Lett.* **2009**, *9*, 2144–2148.
[12] S. D. Evans, S. R. Johnson, Y. L. Cheng, T. Shen, *J. Mater. Chem.* **2000**, *10*, 183–188.
[13] Y. Kim, R. C. Johnson, J. T. Hupp, *Nano Lett.* **2001**, *1*, 165–167.
[14] H.-L. Zhang, S. D. Evans, J. R. Henderson, R. E. Miles, T.-H. Shen, *Nanotechnology* **2002**, *13*, 439–444.
[15] Y. Zhou, S. Wang, K. Zhang, X. Jiang, *Angew. Chem.* **2008**, *120*, 7564–7566; *Angew. Chem. Int. Ed.* **2008**, *47*, 7454–7456.
[16] M. Riskin, R. Tel-Vered, T. Bourenko, E. Granot, I. Willner, *J. Am. Chem. Soc.* **2008**, *130*, 9726–9733.
[17] X. Zhang, Q. Guo, D. Cui, *Sensors* **2009**, *9*, 1033–1053.
[18] D. A. Schultz, *Curr. Opin. Biotechnol. Curr. Opin. Biotech.* **2003**, *14*, 13–22.
[19] C. M. Niemeyer, *Angew. Chem.* **2003**, *115*, 5974–5978; *Angew. Chem. Int. Ed.* **2003**, *42*, 5796–5800.
[20] E. Katz, I. Willner, *Angew. Chem.* **2004**, *116*, 6166–6235; *Angew. Chem. Int. Ed.* **2004**, *43*, 6042–6108.
[21] N. L. Rosi, C. A. Mirkin, *Chem. Rev.* **2005**, *105*, 1547–1562.
[22] J. F. Hainfeld, R. D. Powell, *J. Histochem. Cytochem.* **2000**, *48*, 471–480.
[23] R. Wilson, *Chem. Soc. Rev.* **2008**, *37*, 2028–2045.
[24] A. Corma, H. Garcia, *Chem. Soc. Rev.* **2008**, *37*, 2096–2126.
[25] C. Della Pina, E. Falletta, L. Prati, M. Rossi, *Chem. Soc. Rev.* **2008**, *37*, 2077–2095.
[26] R. Lévy, N. T. K. Thanh, R. C. Doty, I. Hussain, R. J. Nichols, D. J. Schiffrin, M. Brust, D. G. Fernig, *J. Am. Chem. Soc.* **2004**, *126*, 10076–10084.
[27] D. Aili, M. M. Stevens, *Chem. Soc. Rev.* **2010**, *39*, 3358.
[28] M. Brust, M. Walker, D. Bethell, D. J. Schiffrin, R. Whyman, *J. Chem. Soc. Chem. Commun.* **1994**, 801–802.
[29] X.-M. Li, M. R. de Jong, K. Inoue, S. Shinkai, J. Huskens, D. N. Reinhoudt, *J. Mater. Chem.* **2001**, *11*, 1919–1923.
[30] E. J. Shelley, D. Ryan, S. R. Johnson, M. Couillard, D. Fitzmaurice, P. D. Nellist, Y. Chen, R. E. Palmer, J. A. Preece, *Langmuir* **2002**, *18*, 1791–1795.
[31] T. Peterle, A. Leifert, J. Timper, A. Sologubenko, U. Simon, M. Mayor, *Chem. Commun.* **2008**, 3438–3440.
[32] T. Peterle, P. Ringler, M. Mayor, *Adv. Funct. Mater.* **2009**, *19*, 3497–3506.

[33] J. P. Hermes, F. Sander, T. Peterle, C. Cioffi, P. Ringler, T. Pfohl, M. Mayor, *Small* **2011**, *7*, 920–929.
[34] J. P. Hermes, F. Sander, T. Peterle, M. Mayor, *CHIMIA* **2011**, *65*, 219–222.
[35] F. Sander, T. Peterle, N. Ballav, F. von Wrochem, M. Zharnikov, M. Mayor, *J. Phys. Chem. C* **2010**, *114*, 4118–4125.
[36] H.-M. Huang, C.-Y. Chang, I.-C. Liu, H.-C. Tsai, M.-K. Lai, R. C.-C. Tsiang, *J. Polym. Sci., Part A: Polym. Chem.* **2005**, *43*, 4710–4720.
[37] I. Hussain, S. Graham, Z. Wang, B. Tan, D. C. Sherrington, S. P. Rannard, A. I. Cooper, M. Brust, *J. Am. Chem. Soc.* **2005**, *127*, 16398–16399.
[38] D. Wan, Q. Fu, J. Huang, *J. Appl. Polym. Sci.* **2006**, *101*, 509–514.
[39] Z. Wang, B. Tan, I. Hussain, N. Schaeffer, M. F. Wyatt, M. Brust, A. I. Cooper, *Langmuir* **2007**, *23*, 885–895.
[40] A. Taubert, U.-M. Wiesler, K. Müllen, *J. Mater. Chem.* **2003**, *13*, 1090–1093.
[41] G. Bergamini, P. Ceroni, V. Balzani, M. Gingras, J.-M. Raimundo, V. Morandi, P. G. Merli, *Chem. Commun.* **2007**, 4167.
[42] A. D'Aléo, R. M. Williams, F. Osswald, P. Edamana, U. Hahn, J. van Heyst, F. D. Tichelaar, F. Vögtle, L. De Cola, *Adv. Funct. Mater.* **2004**, *14*, 1167–1177.
[43] Y. Hosokawa, S. Maki, T. Nagata, *Bull. Chem. Soc. Jpn.* **2005**, *78*, 1773–1782.
[44] E. Boisselier, A. K. Diallo, L. Salmon, C. Ornelas, J. Ruiz, D. Astruc, *J. Am. Chem. Soc.* **2010**, *132*, 2729–2742.
[45] K. Esumi, A. Kameo, A. Suzuki, K. Torigoe, *Colloids Surf. A* **2001**, *189*, 155–161.
[46] J. D. Gilbertson, G. Vijayaraghavan, K. J. Stevenson, B. D. Chandler, *Langmuir* **2007**, *23*, 11239–11245.
[47] M. Pittelkow, T. Brock-Nannestad, K. Moth-Poulsen, J. B. Christensen, *Chem. Commun.* **2008**, 2358–2360.
[48] R. M. Crooks, M. Zhao, L. Sun, V. Chechik, L. K. Yeung, *Acc. Chem. Res.* **2001**, *34*, 181–190.
[49] J. J. Michels, J. Huskens, D. N. Reinhoudt, *J. Chem. Soc., Perkin Trans. 2* **2002**, 102–105.
[50] H.-F. Chow, M.-K. Ng, C.-W. Leung, G.-X. Wang, *J. Am. Chem. Soc.* **2004**, *126*, 12907–12915.
[51] A. Dahan, A. Weissberg, M. Portnoy, *Chem. Commun.* **2003**, 1206–1207.
[52] A. Dahan, M. Portnoy, *J. Am. Chem. Soc.* **2007**, *129*, 5860–5869.
[53] A. Van Bierbeek, M. Gingras, *Tetrahedron Lett.* **1998**, *39*, 6283–6286.
[54] W. M. Pankau, S. Mönninghoff, G. von Kiedrowski, *Angew. Chem.* **2006**, *118*, 1923–1926; *Angew. Chem. Int. Ed.* **2006**, *45*, 1889–1891.
[55] W. Offermann, F. Vögtle, *Synthesis* **1977**, *1977*, 272–273.
[56] R. C. Fuson, B. Freedmann, *J. Org. Chem.* **1958**, *23*, 1161–1166.
[57] C.-C. Han, R. Balakumar, *Tetrahedron Lett.* **2006**, *47*, 8255–8258.
[58] M. M. Alvarez, J. T. Khoury, T. G. Schaaff, M. N. Shafigullin, I. Vezmar, R. L. Whetten, *J. Phys. Chem. B* **1997**, *101*, 3706–3712.
[59] M. J. Hostetler, J. E. Wingate, C.-J. Zhong, J. E. Harris, R. W. Vachet, M. R. Clark, J. D. Londono, S. J. Green, J. J. Stokes, G. D. Wignall, G. L. Glish, M. D. Porter, N. D. Evans, R. W. Murray, *Langmuir* **1998**, *14*, 17–30.
[60] P. J. Magelhaes, S. J. Ram, M. D. Abramoff, *Biophotonics Int.* **2004**, *11*, 36–42.
[61] R. Wilson, Y. Chen, J. Aveyard, *Chem. Commun.* **2004**, 1156.
[62] C. Krüger, S. Agarwal, A. Greiner, *J. Am. Chem. Soc.* **2008**, *130*, 2710–2711.
[63] P. D. Jadzinsky, G. Calero, C. J. Ackerson, D. A. Bushnell, R. D. Kornberg, *Science* **2007**, *318*, 430–433.
[64] M. W. Heaven, A. Dass, P. S. White, K. M. Holt, R. W. Murray, *J. Am. Chem. Soc.* **2008**, *130*, 3754–3755.
[65] D. Thompson, J. P. Hermes, A. Quinn, M. Mayor, in preparation.

Received: June 16, 2011
Published online: October 26, 2011

